Influence of the structural sealant joints on the blast performance of laminated glass panels

Hasitha D. Hidallana-Gamage[1], David P. Thambiratnam[2], Nimal J. Perera[3]

Abstract: This paper investigates the influence of structural sealant joints on the blast performance of laminated glass (LG) panels, using a comprehensive numerical procedure. A parametric study was carried out by varying the width, thickness and the Young's modulus (E) of the structural silicone sealant joints and the behavior of the LG panel was studied under two different blast loads. Results show that these parameters influence the blast response of LG panels, especially under the higher blast load. Sealant joints that are thicker, have smaller widths and lower E values increase the flexibility at the supports and hence increase the energy absorption of the LG panel while reducing the support reactions. Results also confirmed that sealant joints designed according to current standards perform well under blast loads. Modeling techniques presented in this paper could be used to complement and supplement the guidance in existing design standards. The new information generated in this paper will contribute towards safer and more economical designs of entire facade systems including window glazing, frames and supporting structures.

Keywords: Laminated glass; Blast loads; Finite element modeling; Parametric study; Sealant properties; Energy absorption; Support reactions

---

[1]Ph. D. Student, Faculty of Science & Engineering, Queensland University of Technology, GPO Box 2434, 2 George St., Brisbane, Queensland 4001. E-mail: hasithagamage@yahoo.com

[2]Professor, Faculty of Science & Engineering, Queensland University of Technology, GPO Box 2434, 2 George St., Brisbane, Queensland 4001. E-mail: d.thambiratnam@qut.edu.au.

[3]Adjunct Professor, Faculty of Science & Engineering, Queensland University of Technology, GPO Box 2434, 2 George St., Brisbane, Queensland 4001. E-mail: nimal.perera@robertbird.com.au

Introduction

Building facades form the skin of a building and are very vulnerable to damage during blast events. Glazed facades are frequently used in buildings because of their architectural features and aesthetical aspects. These glazed facades could be 4-10 m high at the lower levels of the buildings which are the most affected by explosions occurring at the ground level. Past terrorist attacks showed that most of the blast related injuries occurred directly and indirectly from window glass failure (Norville et al. 1999). These injuries can be classified into three types as primary, secondary and tertiary (Lin et al. 2004). The injuries such as eardrum rupture and lung collapse are the primary injuries which could occur due to the air blast pressure entering the building through the broken glass windows. Lacerations and blunt trauma are the secondary injuries which could occur by broken glass fragments hitting the people. Additionally, building occupants could be thrown against objects by the force of the explosion causing tertiary injuries. However, if the building facades are designed for a credible blast load, they could minimize these hazards from at least moderate size terrorist attacks that do not cause structural failure.

Different blast mitigation and window retrofit techniques such as window films, catch systems, window replacement systems, installation of secondary windows, and or a combination of these systems are used in practice to mitigate blast hazards (Lin et al. 2004). Window film is the most economical solution, but provides the least blast protection. Window catch systems provide adequate blast resistance, but they could disturb building occupants and even affect the appearance of the building. Replacing windows with different glazing types such as laminated glass (LG) and polycarbonate is expensive, but provides the greatest level of protection. LG absorbs the blast energy, unlike monolithic glass, and avoids free flying shards as the interlayer holds the glass fragments upon fracture. LG is more

flexible than polycarbonate and hence transfers comparatively less forces to the window frame and supporting structure. The use of LG in blast resistant glazing could be a safe and economical solution for the potential terrorist attacks.

LG consists of two or more glass plies permanently bonded with one or more polymer interlayers. Annealed and heat strengthened glass types are usually used in LG instead of fully tempered glass as they provide large shards upon fracture which adhere well to the interlayer reducing the amount of flying and falling glass shards (Norville and Conrath 2001). Polyvinyl butyral (PVB) is the common interlayer material used in LG, but some stiffer interlayer materials such as ionoplast are also used in practice (Ledbetter et al. 2006). LG panels are fixed to the window frames using structural sealant joints where silicone and rubber are the common sealant materials. LG panels should be designed to fail by tearing of the interlayer rather than any failure at the supports under the designed blast load. They should be able to absorb blast energy while transferring lesser forces and energy to the window frames and supporting structures. From this aspect, structural sealant joints will have a considerable influence on the blast performance of LG panels and this will be the focus of the present study.

This paper presents a comprehensive numerical procedure to study the blast response of LG panels using the LS-DYNA finite element (FE) code. A parametric study is carried out by varying the width, thickness and the Young's modulus (E) of the structural sealant joints to investigate their influence on the performance of the LG panel under different blast loads. Results from the FE analysis indicate that the geometric and material properties of structural sealant joints have considerable influence on the energy absorption as well as the support reactions of the LG panel. If the sealant joints are under designed, they will fail before the LG panel reaches its capacity by tearing of the interlayer, and hence the entire unit will be flung into the building creating a significant hazard. On the contrary, if they are over designed by

using wider joints or stiffer material, they will transfer higher loads to the supporting window frames. The research information and the modeling techniques presented in this paper could be used to complement and supplement the guidance in current design standards and will enable engineers to better design LG for a credible blast event by maximizing their energy absorption while minimizing the support reactions. This will contribute towards safer and more economical design of the entire façade system including window glazing, frames and supporting structures.

Background

The most challenging part of designing blast resistant structures is to estimate the credible blast load as the type, magnitude and location of the explosions caused by terrorist attacks will be unknown. Hence, the blast load used in the design should be realistic and also the blast resistant design achievable. This section provides some background information on the blast phenomenon and the methods of estimating the blast related parameters. Current design standards and test methods for blast resistant glazing and their limitations are then briefly discussed.

Blast phenomenon

A blast or explosion releases energy suddenly by generating hot gases under high pressure and temperature. Blast overpressure could be high as 30 MPa and the temperature could increase up to 3000-4000 C° (Ngo et al. 2007). High pressure gas travels away from the explosion source at a high velocity by creating shock waves. Initially, the pressure of the shock front increases to a maximum overpressure and then decays as the shock wave expands away from the explosion source. After a short time, pressure behind the shock front drops below the ambient pressure by creating a partial vacuum. It creates high suction winds capable of carrying debris for long distances away from the explosion source.

A typical blast overpressure time-history curve at a point away from the blast source is illustrated in Fig. 1. After the blast, air pressure at a particular point increases suddenly to a peak value then decreases gradually and goes through a negative period. This blast overpressure time profile can be mathematically represented by the Friedlander equation (Wei et al. 2006; UFC 2008), as given by Eq. (1), where P(t) is the instantaneous overpressure at time t, P_{amb} is the ambient pressure, P_{max} is the peak pressure when $t = 0$, $P_{op} = (P_{max} - P_{amb})$ is the peak overpressure at $t = 0$, t_o is the positive pressure duration and b is the decay factor.

$$P(t) = P_{op}(1 - t/t_o)e^{-bt/t_o} \quad (1)$$

Blast wave properties such as peak reflected overpressure, positive load duration and positive reflected impulse depend on charge weight and standoff distance. Hopkinson-Cranz or cube root method is widely used in scaling blast loads and is presented by Eq. (2) (Ngo et al. 2007; Silva and Lu 2009), where Z is the scaled distance in $m/kg^{1/3}$, R is the standoff distance in m and W is the charge weight in kg. However, when both R and W are obtained in ft and lb respectively, Z is calculated in $ft/lb^{1/3}$.

$$Z = R/W^{1/3} \quad (2)$$

Different methods such as empirical methods, mathematical equations and numerical methods are available to estimate blast related parameters. In the present study blast related parameters are evaluated using the empirical method given in UFC 3-340-02 (UFC 2008). For a given charge weight and a standoff distance, the scaled distance, Z is calculated in $ft/lb^{1/3}$ and the relevant chart given in UFC 3-340-02 (UFC 2008) is used to determine the peak reflected overpressure, positive load duration and positive reflected impulse of the blast load. In this paper, these parameters are calculated using the chart developed for blasts occurring from hemispherical trinitrotoluene (TNT) explosions on the surface at sea level

(UFC 2008). Only the positive phase of the blast load is considered in this study whereas the negative phase will have some influence on flexible structures such as cable net facades (Teich et al. 2011). The blast overpressure time-history curve was obtained using the Friedlander equation given in Eq. (1).

Design standards for blast resistant glazing

American Society for Testing and Materials (ASTM) F 2248-09 (ASTM 2010), Unified Facilities Criteria (UFC) 4-010-01 (UFC 2013), UFC 3-340-02 (UFC 2008) and UK Glazing Hazard Guide (1997) are the latest standards used in designing glazed facades to blast loads. These standards are briefly described below.

ASTM F 2248-09 (ASTM 2010)

The ASTM F 2248-09 (ASTM 2010) provides a structured procedure to design glass facades using LG or insulated glass fabricated with LG to blast loads. If the charge weight and the standoff distance are known, the 3-second duration equivalent design load could be found from the ASTM F 2248-09. Then the required thickness of LG could be found by referring to the relevant chart given in ASTM E 1300-09a (ASTM 2009). The design charts available in ASTM E 1300-09a were developed only for LG panels with PVB interlayer. Performance of LG panels with different interlayer materials and thicknesses are not accounted for in this standard. Moreover, these design charts could only be used to design relatively smaller LG panels having a maximum length of about 5 m and width of about 4 m.

ASTM F 2248-09 recommends using either structural silicone sealant or adhesive glazing tape to fix glazing to the supporting frame. The structural silicone sealant joints should have at least 5 mm thickness. The width (bite) of the structural silicone sealant joints should be at least equal to or greater than 10 mm or the nominal thickness of the glass panes, but less than

144 twice the nominal thickness of glass panes to which it adheres. The glazing tape should be
145 within two to four times the thickness of the glass pane. Framing members are designed to
146 withstand a load twice the load resistance of the attached glazing, and edge deflection of the
147 glazing should be less than L/60, where L denotes the length of the supported edge.

148 ***Facilities Criteria (UFC) standards***

149 Department of Defense (DOD), United States has developed Unified Facilities Criteria (UFC)
150 standards which are used in blast resistant glazing design. UFC 4-010-01 (UFC 2013) and
151 UFC 3-340-02 (UFC 2008) are two such standards and these are described below. UFC 4-
152 010-01 (UFC 2013) recommends using LG in blast resistant glazing and it should be
153 designed for a credible blast load using dynamic analysis, testing or the approach given in
154 ASTM F 2248-09. Dynamic analysis could be carried out using FE codes or the simpler
155 computer programs recognized by the blast community. Blast testing is expensive, creates
156 health and safety issues and environmental pollution which makes it difficult in practice. In
157 addition to LG, polycarbonate windows could also be used in blast resistant glazing where
158 the width of structural sealant joints should be no less than 1.5 times the polycarbonate
159 thickness. UFC 3-340-02 (UFC 2008) provides guideline to design blast resistant glazing
160 with monolithic fully tempered glass only.

161 ***UK Glazing Hazard Guide***

162 The U.K. Glazing Hazard Guide (1997) provides a more realistic approach to design blast
163 resistant glazing with LG by accounting for their post-crack load carrying capacity. It
164 provides a set of diagrams called Pressure-Impulse diagrams (P-I diagrams) to evaluate the
165 performance of LG panels under a given blast loading. The panel edges should be securely
166 held in robust frames by using structural silicone sealant joints with a width (bite) of about 35
167 mm. Support reactions should be obtained based on equivalent SDOF factors for two-way

spanning simply supported panes with a uniform load. However, guidelines given in this standard are valid only for a few window sizes used in the UK and are not applicable elsewhere. The U.K. Glazing Hazard Guide is a highly confidential document which is restricted to military use.

Standard test methods for blast resistant glazing

Standard test methods provide guideline to classify the hazard rating of glazed panels depending on their performance under blast loads. These test methods can be classified into two types as arena air blast test and shock tube test. An arena air blast test is carried out in an open environment and a shock tube test is carried out in a closed tube. ASTM F 1642-04 (ASTM 2010b) test method facilitates both arena air blast and shock tube tests. International Organization for standardization (ISO) provides two standard test methods that could be used to test and classify the performance of glazing systems under blast loads. They are ISO 16933 (ISO 2007a) and ISO 16934 (ISO 2007b) where the former is based on arena air blast test while the latter is based on shock tube test. These ASTM and ISO standards provide a structured procedure to test security glazing including, those fabricated from glass, plastic glazing sheet materials, glass-clad plastics, LG, insulated glass, glass/plastic glazing materials, and film-backed glass.

Blast testing is very expensive and hence out of reach of most design engineers. Most of the universities and government organizations do not have adequate funds and facilities to conduct blast testing. These test methods require repetitive testing to accurately predict the behavior and the failure of a glazed panel under a blast load. On the other hand, these test methods are valid for small test specimens with standard dimensions. Large glazed panels used in most buildings could not be classified to suit the above standards. Health and safety issues and environmental pollution are some other negative effects of blast testing.

Computer programs for blast resistant glazing design

Dynamic analysis and design of blast resistant glazing could be carried out by using the computer programs recognized by the blast community. Window Glazing Analysis Response and Design (WinGARD) and Single-degree-of-freedom Blast Effects Design Spreadsheet (SBEDS-W) are two such computer programs used in practice. These programs are based on SDOF analysis where the approach is an iterative process of selecting initial glazing or member size and then repeating the analysis until the window system is found to have an acceptable response. They accept user inputs of window system properties and explosion characteristics, and then evaluate the performance of the window system under the defined blast load. They could display the results graphically or in text format including key parameters such as displacements, fragment flight and support reactions. These programs however have some limitations. One of the major limitations is that the design outcomes may not be realistic as they are based on a simplified SDOF analysis. These programs generate the output results either graphically or as a text summary unlike in the FE codes where it is possible to observe the predicted response and the failure pattern.

Influence of structural sealant joints

Structural sealant joints play an important role in a LG panel as they should be able to withstand the designed blast load, while transferring less force to the supporting frame. Design standards such as ASTM F 2248-09 (ASTM 2010) provides some useful information to design the required width and thickness of the structural sealant joints. However, research has not been carried out to investigate the influence of the structural sealant joints, in-terms of their width, thickness and the material properties on the blast performance of LG panels. This could be an important and timely topic as it is not addressed properly in the current design standards and the research to date. Blast testing could be an option for such investigations,

but it has numerous limitations as discussed earlier. This emphasizes the need for a new analytical procedure to study the blast response of LG panels and the influence of the structural sealant joints. Numerical analysis with FE codes is a feasible method that has been used to investigate the behavior of LG panels under blast loads and this approach is presented below.

Finite element modeling and analysis of LG

LG has a small thickness compared to its in-plane dimensions and could be modeled with either two dimensional (2D) shell elements or three dimensional (3D) solid elements. Blast response of LG has been studied using FE codes having explicit capabilities such as LS-DYNA, ABAQUS, ANSYS and EUROPLEXUX (Chung et al. 2010; Weggel and Zapata 2008; Seica et al. 2011). However, most of the past research has some limitations and these are explained below in the paper. The modeling techniques used by the authors to overcome those limitations are then presented.

Limitations in the research to date

It is well-known that post-crack load carrying capacity of LG is considerably higher than that at the pre-crack stage. However, most of the research using FE techniques has been unable to account for the damage strength of glass and hence the post-crack behavior of LG. In addition, few researchers accounted for the structural sealant joints when modeling LG panels, while most used simplified support conditions. Research has been carried out by modeling sealant joints with three linear springs representing in-plane, normal and rotational stiffness at each node (Weggel and Zapata 2008). However, that model has some limitations since the spring constants are available only for sealant joints with limited dimensions.

This paper investigates the effects of structural sealant joints on the blast response of LG panels by varying their width, thickness and material properties. This type of investigation requires a complete 3D model of LG including glass, interlayer and sealant joints, as the 2D models will be unable capture the realistic support conditions (Hidallana-Gamage et al. 2013a). The authors have developed a rigorous and a reliable numerical procedure to study the blast response of LG by overcoming the limitations described above. These modeling techniques are briefly described in this paper and were described in detail in their previous research work (Hidallana-Gamage et al. 2013a, b).

Present modeling techniques

In the present study, the entire LG panel, consisting of glass, interlayer and silicone joints, is modelled with 3D constant stress solid elements using LS-DYNA FE code (Hallquist 2006). The contact between the glass and PVB was treated as fully bonded and hence there cannot be any delamination between glass panes and PVB interlayer. However, severely damaged glass elements were allowed to delete from the FE model by selecting the failure strain to be 0.0024 in the analysis. The contact between the glass and sealant joints was also treated as fully bonded. Glass is modeled with material model 110 (MAT_HOLMQUIST_CERAMICS) and both interlayer and structural sealant joints are modeled with material model 24 (MAT_PIECEWISE_LINEAR_PLASTICITY). The window frame is modeled as a rigid base by neglecting its deformations for simplicity. The material models used for glass, interlayer and sealant joints are briefly described below.

Material model for glass

The material model 110 which is used for glass was developed based on Johnson-Holmquist (JH-2) material model which has been widely used to model brittle materials such as glass, ceramic, concrete and rock subjected to high pressures, large strains and high strain rates. The

JH-2 material model was developed with a set of mathematical equations and they are explained in detail in the literature (Holmquist et al. 1995). This material model provides a realistic approach in modeling the behavior of glass by reducing its strength depending on the damage level. The normalized equivalent stress (σ^*) of the material is determined using the normalized intact equivalent stress (σ^*_i), normalized fracture stress (σ^*_f) and material damage (D) as given by Eq. (3), where all the stresses are normalized by dividing them by σ_{HEL}, which is the stress at Hugoniot Elastic Limit (HEL).

$$\sigma^* = \sigma^*_i - D\,(\sigma^*_i - \sigma^*_f) \tag{3}$$

Material model for interlayer and sealant joints

Interlayer materials such as PVB and ionoplast show viscoelastic behavior under loads with long durations where their shear modulus changes with the time. However, when the load duration is small (about 100 ms or less) as observed under blast loads, the change in the shear modulus of polymeric interlayers is negligible and hence they could be analyzed as an elastic-plastic material (Larcher et al. 2012; Hidallana-Gamage et al. 2013a, b; Wei and Dharani 2006). Silicone and rubber are the common sealant materials and their behavior could also be treated as elastic-plastic under blast loads. Material model 24 is widely used to model polymeric materials with elastic-plastic properties and hence it is used to model both interlayer and sealant materials. The authors have confirmed the validity of these material models to analyze the behavior of LG under blast loads in their previous research work (Hidallana-Gamage et al., 2013a, b).

Failure analysis of materials

The failure theories used in the present study to analyze the failure of glass, interlayer and sealant materials are briefly described in the paper. For brittle materials such as glass the 1st principal stress (σ_{11}) is usually used to examine the failure. Glass is considered to have failed

285 if the σ_{11} exceeds the dynamic breaking strength of glass (T_b) which could increase up to 80
286 MPa for annealed glass under blast loads (Hooper et al. 2012; Seica et al. 2011). However,
287 glass is not a homogeneous material and could break at strengths lower than the expected
288 theoretical values due to the presence of surface flaws and micro cracks.

289 Both the interlayer and sealant materials show ductile behavior and the von mises stress (σ_v)
290 is used to examine their failure. In the present study, they are considered to have failed if the
291 σ_v exceeds the failure stress of the material. The authors have explained these failure theories
292 and their application to the FE modeling in detail in their previous research work (Hidallana-
293 Gamage et al. 2013b).

294 Modelling, parametric study and results

295 A LG panel with a length of 1.1 m, width of 0.9 m and a thickness of 7.52 mm (3 mm
296 annealed glass + 1.52 mm PVB + 3 mm annealed glass) was used for the study. According to
297 ASTM F 2248-09 (ASTM 2010a), LG panel should be fixed to the frame using structural
298 silicone sealant joints having a minimum thickness of 5 mm and a width (bite) of 10-12 mm.
299 Initially, the width and the thickness of the structural sealant joints were taken as 10 and 5
300 mm respectively. Detailed information on the blast loads, FE model and the material
301 properties used in the analysis is presented below. The performance of the LG panel was
302 examined under two different blast loads and then a parametric study was carried out by
303 varying the width, thickness and the Young's modulus (E) of the structural sealant joints.

304 Blast loads

305 The performance of the LG panel was examined under two different blast loads. Blast load 1
306 is the weaker blast load generated from 18 kg TNT equivalent charge weight at 25 m stand-
307 off distance and blast load 2 is the stronger blast load generated form the same charge weight

at 15 m stand-off distance. Blast wave parameters were calculated according to UFC 3-340-02 (UFC 2008) as described earlier in the paper. Blast load 1 has a reflected overpressure of about 31 kPa, positive load duration (t_o) of about 12.3 ms and a reflected impulse of about 150 kPa-ms and the corresponding parameters for blast load 2 are 70 kPa, 10.3 ms and 270 kPa-ms respectively. The blast overpressure time-history curves were obtained from the Friedlander equation and the relevant decay factors (b) for the blast loads 1 and 2 were found to be 0.79 and 0.94 respectively. The reflected blast overpressure time history curves used in the analysis are shown in Fig. 2.

FE modeling

In the present study, the entire LG panel, consisting of glass, interlayer and silicone joints, was modelled with 3D constant stress solid elements using LS-DYNA FE code (Hallquist 2006) as was explained earlier. The sealant joints were fixed to a rigid base neglecting the deformations in the frame for simplicity. This could be a conservative approach as the flexible window frames could absorb some energy reducing the damage to the LG panel (Weggel and Zapata 2008). The blast load was assumed to be uniformly distributed over the entire front glass pane and hence only one-quarter of the LG panel was analyzed by accounting for the symmetry of the model and loading. Convergence was established and a FE model with 220 x 180 x 10 elements (along length x width x thickness) was used in the analysis where each glass layer and the PVB interlayer were modelled with 4 and 2 elements respectively through the thickness. A 3D view and a sectional view at the supports of the FE model are shown in Fig. 3(a and b) respectively.

Material Properties

The material properties of glass and the JH-2 material constants required for the material model 110 were obtained from the literature (Holmquist et al. 1995; Hooper et al. 2012) and

those used in the analysis are presented in Table 1. The density, Young's modulus (E) and Poisson's ratio of glass were taken as 2530 kg/m^3, 72 GPa and 0.22 respectively (Hooper et al. 2012). The tensile strength (T) of glass used with the material model 110 should be about 60-65 MPa for annealed glass (Hidallana-Gamage et al. 2013a, b) and it was taken as 60MPa in the analysis as a conservative approach.

The material properties of the PVB interlayer and structural silicone sealant joints are summarized in Table 2. The density, Young's modulus (E) and Poisson's ratio of the PVB interlayer were taken as 1100 kg/m^3, 530 MPa and 0.485 respectively (Hooper et al. 2012). PVB was treated as an elastic-plastic material where its yield stress, failure stress and failure strain were taken as 11 MPa, 28 MPa and 2.0 respectively (Larcher et al. 2012).

The density and Poisson's ratio of silicone sealant were taken as 1100 kg/m^3 and 0.495 respectively. The Young's Modulus E of the silicone sealant was taken as 2.3 MPa by assuming that it has a hardness of about 50 IRHD in accordance with ISO 48 (ISO 1994) and its yield stress, failure stress and failure strain were taken as 2.3 MPa, 3.5 MPa and 2.5 respectively. This paper investigates the effects of the stiffness of the structural sealant joints and hence E of silicone sealant was varied between 1.5-3.4 MPa in the analysis by assuming that its hardness varies between 40-60 IRHD. The yield stress and the failure stress of sealant were also changed proportionally with the change of E.

Comparison of results

The behavior of the LG panel was compared under the chosen blast loads. Results from the FE analysis for mid-span deflection, fracture pattern of the glass panes, stresses of different components and support reactions are presented below.

Mid-span deflection

Fig. 6 compares the deflection time-history curves at the center of the LG panel for the two chosen blast loads. It is evident that the two responses are quite different, as expected. Maximum deflection observed under the weaker blast load is about 34 mm at 12 ms and that observed under the stronger blast load is about 110.6 mm at 15 ms. There is approximately a 300% increase in the maximum deflection under the stronger blast load. LG panel shows a rebound under the weaker blast load confirming that little damage has occurred to the glass panes. On the other hand, LG panel does not show any rebound under the stronger blast load indicating that significant damage could have occurred to the glass panes.

Energy absorption

It is important to maximize the energy absorption when designing LG under blast loads. The total energy absorbed by the FE models is compared under different blast loads in Fig. 5. The energy absorption responses under both blast loads steadily increase and reach their maximum values during 8-10 ms and then remain constant thereafter. The maximum energy absorbed under the stronger blast load is about 279.1 J which is considerably higher than that observed under the weaker blast load which is about 63.2 J. When the deflection increases, the LG panel absorbs more energy and hence shows an increase in the energy absorption under the stronger blast load. The energy absorption response is used to evaluate the performance of the LG panel during the parametric study later in the paper.

Fracture and crack propagation in glass panes

Fig.6(a and b) show the fracture and crack propagation in the front and back glass panes under the weaker blast load at 12 ms. Those under the stronger blast load at 15 ms are shown in Fig. 7(a and b). The back glass panes have more cracks compared to the front glass panes under both blast loads as they attract larger tensile stresses when the LG panels deform inwards under the blast loads. Glass is weak in tension and the glass elements in the FE

model fail under excessive plastic strains. The LG panel has a larger deflection and energy absorption under the stronger blast load and hence both glass panes fractured and have more cracks than those under the weaker blast load.

Stress-strain behavior of the interlayer

Fig. 8(a) shows the plastic strain variation on the bottom surface of the interlayer under the weaker blast load at 12 ms. The von mises stress (σ_v) is used to examine the failure of the interlayer as described earlier in the paper. PVB elements have exceeded their yield stress which is about 11 MPa along the yield lines, but most of the elements have a σ_v less than 20 MPa showing no sign of damage to the interlayer under the weaker blast load. Fig. 8(b) shows the plastic strain variation on the bottom surface of the interlayer under the stronger blast load at 15 ms. There is an increase in the length and width of the yield lines under the stronger blast load. Most of the PVB elements along the yield lines have a σ_v more than 20 MPa and a few PVB elements at four locations highlighted in Fig. 8(b) has reached their failure stress which is about 28 MPa. The interlayer has torn at those locations under the stronger blast load implying that this blast load could be much closer to the design capacity of the LG panel.

Stress analysis of sealant joints

The variation of σ_v in the structural sealant joints was examined under the blast loads. Sealant joints at the middle of both the long and short edges have high stresses compared to other parts, but the stress at the middle of the long edge is slightly higher than that at the short edge. Fig. 9 compares the variation of σ_v in critical sealant elements at the middle of the long edge under the blast loads. Maximum stress of about 0.85 MPa could be seen at about 10 ms under the weaker blast load. The σ_v is well below the yield stress of the sealant material which is about 2.3 MPa, anywhere in the FE model. Maximum stress observed under the

stronger blast load is about 2.54 MPa at about 7.5 ms, which is more than the yield stress, but less than the failure stress of about 3.5 MPa. Sealant joints are hence in the elastic region under the weaker blast load and they are in the plastic region under the stronger blast load.

Support Reactions

The stresses of sealant joints along the perimeter of the LG panel were examined as they provide an indication of the forces transferred to the supporting frame. As was discussed earlier in this paper sealant elements at the middle of the both long and short edges have slightly high stresses compared to those at other areas. The reaction force per unit length at the middle of the long edge (R_L) and that at the middle of the short edge (R_S) were therefore considered in this study. Magnitudes of the both R_L and R_S were determined using Eq. (4) and (5) respectively, where R_x, R_y and R_z are the reaction forces per unit length in the directions of X, Y and Z respectively at the supporting edges (refer Fig. 3). The reaction forces in the plane of the panel (R_x, R_y) and that perpendicular to the panel (R_z) were therefore treated to calculate the R_L and R_S. However, it has to be noted that these reaction forces vary along the edges though only those at the middle of the edges were treated in this study. Furthermore, window frame and their attachments to the walls were not treated in this study which gives a conservative approach as these members could absorb some energy and reduce the support reactions.

$$R_L = (R_y^2 + R_z^2)^{1/2} \quad (4)$$

$$R_S = (R_x^2 + R_z^2)^{1/2} \quad (5)$$

Fig. 10(a) compares the variations of support reactions at the middle of the long and short edges (R_L and R_S) under the weaker blast load. Both R_L and R_S show a similar variation where they suddenly increase to a maximum at about 6-7 ms and gradually reduce thereafter. R_L has a maximum of about 11.3 kN/m which is slightly higher than the maximum of R_S

425 which is about 11 kN/m. Fig. 10(b) compares the variations of R_L and R_S under the stronger
426 blast load. Both R_L and R_S increase to a maximum at about 6-8 ms and then gradually reduce
427 similar to that observed under the weaker blast load. R_L has a maximum of about 12.3 kN/m
428 and is slightly higher than that of R_S which is about 12.2 kN/m. There is a little increase in
429 the support reactions under the stronger blast load compared to those under weaker blast load.
430 R_L is higher than R_S under both blast loads and therefore it is used as a measure of support
431 reactions during the parametric study.

432 Results from FE analysis for mid-span deflection, energy absorption, crack propagation in
433 glass panes, stress-strain behavior of the interlayer and stresses in sealant joints and support
434 reactions were studied to predict the behavior of the LG panel under the chosen blast loads.
435 Glass panes cracked slightly, interlayer yielded but has stresses were well below the failure
436 stress and the sealant joints did not yield under the weaker blast load. Glass panes cracked
437 considerably, interlayer tore at few locations by reaching the failure stress and sealant joints
438 yielded slightly under the stronger blast load. It is therefore evident that little damage has
439 occurred to the LG panel under the weaker blast load, while significant damage has occurred
440 under the stronger blast load which could be close to the design capacity of the LG panel.
441 These two blast loads represents two different scenarios and hence are used in the parametric
442 study presented below.

443 **Parametric study on the effects of structural sealant joints**

444 A parametric study was carried out with the developed FE models by varying the width,
445 thickness and the stiffness of the structural sealant joints. The width of the silicone sealant
446 joints was varied between 7.5-20 mm and their thickness was varied between 4-6 mm. The
447 Young's modulus (E) of silicone sealant was varied between 1.5-3.4 MPa. The effects of
448 these parametric variations on the blast performance of LG panel were investigated. Results

449 from FE analysis for mid-span deflection, energy absorption and support reactions are
450 discussed under the selected blast loads as presented below. The performance of those FE
451 models with varied sealant properties is compared with that having sealant joints with 10 mm
452 width, 5 mm thickness and a E of 2.3 MPa. The results are summarized in Table 3-5 and the
453 calculated percentage errors are given within brackets.

454 ***Effects of the width of the sealant joints***

455 Five different FE models with 7.5, 10, 12.5, 15 and 20 mm wide sealant joints were used in
456 the analysis while taking their thickness and Young's modulus (E) as 5 mm and 2.3 MPa
457 respectively. Results from FE analysis for mid-span deflection, energy absorption and
458 support reaction at the middle of the long edge (R_L) are compared for the chosen blast loads
459 and are summarized in Table 3.

460 *Mid-span deflection*

461 Fig. 11(a) compares the deflection time-history curves at the center of LG panel for different
462 widths of the structural sealant joints under the weaker blast load. The FE model with 10 mm
463 wide sealant joints gives a maximum deflection of about 34 mm and those obtained from the
464 FE models with 7.5, 12.5, 15 and 20 mm wide sealant joints are about 33.2, 32.8, 32.4 and
465 24.5 mm respectively. Deflection time history curves obtained from the FE models with 7.5-
466 15 mm wide sealant joints show similar behavior and their maximum deflections slightly
467 reduces with the increase of the width of the sealant joints. However, when the width of the
468 sealant joints increases to 20 mm, there is a considerable reduction (about 27.9%) of
469 maximum deflection compared to that with 10 mm wide sealant joints.

470 Fig. 11(b) compares the deflection time-history curves at the center of LG panel for different
471 widths of the structural sealant joints under the stronger blast load. The FE model with 10

mm wide sealant joints gives a maximum deflection of about 110.6 mm and those obtained from the FE models with 7.5, 12.5, 15 and 20 mm wide sealant joints are about 131, 100.6, 98.1 and 95.4 mm respectively. When the width of the sealant joints reduces to 7.5 mm there is about 18.4% increase in the maximum deflection compared to that with 10 mm wide sealant joints. On the other hand, when the width of the sealant joints increases to 20 mm there is about 13.7% reduction in the maximum deflection compared to that with 10 mm wide sealant joints. The variation of the mid-span deflection is quite sensitive to the width of the sealant joints for the stronger blast load compared to that under the weaker blast load.

Energy Absorption

Fig. 12(a) compares the energy absorption of the FE models for different widths of the structural sealant joints under the weaker blast load. The FE model with 10 mm wide sealant joints absorbs a maximum energy of about 63.2 J and those obtained from the FE models with 7.5, 12.5, 15 and 20 mm wide sealant joints are about 65.1, 62.4, 62 and 45.6 J respectively. FE models with 7.5-15 mm wide sealant joints absorb similar amounts of energy and their energy absorption slightly reduces with the increase of the width of the sealant joints. There is a considerable reduction (about 27.8%) in the energy absorption when the width of the sealant joints increases to 20 mm compared to that with 10 mm wide sealant joint.

Fig. 12(b) compares the energy absorption of the FE models for different widths of the structural sealant joints under the stronger blast load. The FE model with 10 mm wide sealant joints absorbs a maximum energy of about 279.1 J and those obtained from the FE models with 7.5, 12.5, 15 and 20 mm wide sealant joints are about 290.4, 270.6, 268.4 and 243.3 J respectively. FE models with 7.5-15 mm wide sealant joints absorb similar amounts of energy under the stronger blast load as was seen for the weaker blast load. The energy

496 absorption reduces with the increase of the width of the sealant joints and the reduction is
497 about 12.8% for the FE model with 20 mm wide sealant joints compared to that with 10 mm
498 wide sealant joint.

499 ***Support reaction (R_L)***

500 Fig. 13(a) compares the variation of the support reaction at the middle of the long edge (R_L)
501 for different widths of the sealant joints under the weaker blast load. Maximum values of R_L
502 for all the FE models are summarized in Table 3, but the variation of R_L for FE models with
503 10, 12.5 and 20 mm wide sealant joints are shown in Fig. 13(a). The FE model with 10 mm
504 wide sealant joints has a maximum R_L of about 11.3 kN/m and those obtained from the FE
505 models with 7.5, 12.5, 15 and 20 mm wide sealant joints are about 10.6, 12.6, 12.7 and 12.9
506 kN/m respectively. Initially, R_L increases suddenly and reaches its maximum during 5-8 ms
507 and then it reduces gradually with time, with many fluctuations. The maximum value of R_L
508 increases slightly with the increase of the width of the sealant joints and there is only about
509 14.2% increase in the R_L when the width increases from 10 mm to 20 mm under the weaker
510 blast load.

511 Fig. 13(b) compares the variation of the R_L for FE models with 7.5, 10 and 12.5 mm wide
512 sealant joints under the stronger blast load. The maximum value of R_L is seen during 4-8 ms
513 and that for all the FE models are summarized in Table 3. The FE model with 10 mm wide
514 sealant joints has a maximum R_L of about 12.3 kN/m and those obtained from the FE models
515 with 7.5, 12.5, 15 and 20 mm wide sealant joints are about 11.3, 17.5, 19.2 and 26 kN/m
516 respectively. Results from FE analysis indicate that the R_L is quite sensitive to the width of
517 the sealant joints for the stronger blast load than the weaker blast load. The percentage
518 increases of the R_L for the FE models with 12.5, 15 and 20 mm wide sealant joints are about
519 42.3%, 56.1% and 111.4% respectively compared to that with the 10 mm wide sealant joints.

The use of wider sealant joints considerably increases the forces transferred to the supporting frames under higher blast loads (while reducing the deflections of the LG panel as observed above).

Effects of the thickness of the sealant joints

Three different FE models with 4, 5 and 6 mm thick sealant joints were used in the analysis while taking their width and Young's modulus as 10 mm and 2.3 MPa respectively. Results from FE analysis for mid-span deflection, energy absorption and support reactions (R_L) are compared under the chosen blast loads and are summarized in Table 4.

Mid-span deflection

Fig. 14(a) compares the deflection time-history curves at the center of LG panel for different thicknesses of the structural sealant joints under the weaker blast load. The FE model with 5 mm thick sealant joints gives a maximum deflection of about 34 mm and those obtained from the FE models with 4 and 6 mm thick sealant joints are about 32.8 and 35.7 mm respectively. The variations of the maximum deflection in those FE models are about -3.5% and 5% respectively compared to that with 5 mm thick sealant joints.

Fig. 14(b) compares the deflection time-history curves at the center of LG panel for different thicknesses of the structural sealant joints under the stronger blast load. The FE model with 5 mm thick sealant joints gives a maximum deflection of about 110.6 mm and those obtained from the FE models with 4 and 6 mm thick sealant joints are about 103.7 and 117.1 mm respectively. The variations of the maximum deflection in those FE models are about -6.2% and 5.9% respectively compared to that with 5 mm thick sealant joints. The thickness of the sealant joints has a little effect on the mid-span deflection, but the maximum deflection

slightly increases with the increase in the thickness of the sealant joints under both blast loads.

Energy absorption

Fig. 15(a) compares the energy absorption of the LG panel for different thicknesses of the structural sealant joints under the weaker blast load. The FE model with 5 mm thick sealant joints absorbs a maximum energy of about 63.2 J and those obtained from the FE models with 4 and 6 mm thick sealant joints are about 62.6 and 64.5 J respectively. The variations of the maximum energy absorption in those FE models are about -0.9% and 2.1% respectively compared to that with 5 mm thick sealant joints.

Fig. 15(b) compares the energy absorption of the LG panel for different thicknesses of the structural sealant joints under the stronger blast load. The FE model with 5 mm thick sealant joints absorbs a maximum energy of about 279.1 J and those obtained from the FE models with 4 and 6 mm thick sealant joints are about 273.8 and 288.1 J respectively. The variations of the maximum energy absorption in those FE models are about -1.9% and 3.2% respectively compared to that with 5 mm thick sealant joints. Energy absorption time-history curves are similar, but the FE models with thicker sealant joints absorb slightly more energy compared to those with thinner sealant joints under both blast loads. However, thickness of the sealant joints does not have a considerable impact on the energy absorption of LG panels under blast loads.

Support reaction (R)

Fig. 16(a) compares the variation of R_L of the LG panel for different thicknesses of the sealant joints under the weaker blast load. The FE model with 5 mm thick sealant joints has a maximum R_L of about 11.3 kN/m and those obtained from the FE models with 4 and 6 mm

565 thick sealant joints are about 12.8 and 10.8 kN/m respectively. The variations of R_L in those
566 FE models are about 13.3% and -4.4% respectively compared to that with 5 mm thick sealant
567 joints.

568 Fig. 16(b) compares the variation of R_L of the LG panel for different thicknesses of the
569 sealant joints under the stronger blast load. The FE model with 5 mm thick sealant joints has
570 a maximum R_L of about 12.3 kN/m and those obtained from the FE models with 4 and 6 mm
571 thick sealant joints are about 14.9 and 12.1 kN/m respectively. The variations of R_L are about
572 21.1% and -1.6% respectively compared to that with 5 mm thick sealant joints. It is evident
573 that the FE models with thinner sealant joints have higher reaction force than those with
574 thicker sealant joints under both blast loads. The reduction of the thickness of sealant joints to
575 4 mm considerably increases the R_L, especially under stronger blast loads.

576 **Effects of the Young's modulus (E) of the sealant joints**

577 Three different FE models with sealant joints having Young's moduli of 1.5, 2.3 and 3.4 MPa
578 were used in the analysis while taking their width and thickness as 10 and 5 mm respectively.
579 Results from FE analysis for mid-span deflection, energy absorption and support reactions
580 (R_L) are compared and are summarized in Table 5.

581 ***Mid-span deflection***

582 Fig. 17(a) compares the deflection time-history curves at the center of LG panel for different
583 stiffness of the structural sealant joints under the weaker blast load. The FE model with
584 sealant joints having E of 2.3 MPa gives a maximum deflection of about 34 mm and those
585 obtained from the FE models with sealant joints having E of 1.5 and 3.4 MPa are about 35
586 and 33.4 mm respectively. The variations of the maximum deflection in those FE models are
587 about 2.9% and -1.8% respectively compared to that with sealant joints having E of 2.3 MPa.

588 Fig. 17(b) compares the deflection time-history curves at the center of LG panel for different
589 stiffness of the structural sealant joints under the stronger blast load. The FE model with
590 sealant joints having E of 2.3 MPa gives a maximum deflection of about 110.6 mm and those
591 obtained from the FE models with sealant joints having E of 1.5 and 3.4 MPa are about 113.8
592 and 103.7 mm respectively. The variations of the maximum deflection in those FE models are
593 about 2.9% and -6.2% respectively compared to that with sealant joints having E of 2.3 MPa.
594 Overall, E of sealant joints has little impact on the mid-span deflection of the LG panel under
595 the treated blast loads.

596 ***Energy absorption***

597 Fig. 18(a) compares the energy absorption of the LG panel for different stiffness of the
598 structural sealant joints under the weaker blast load. The FE model with sealant joints having
599 E of 2.3 MPa absorbs a maximum energy of about 63.2 J and those obtained from the FE
600 models with sealant joints having E of 1.5 and 3.4 MPa are about 65.3 and 62.5 J
601 respectively. The variations of the maximum energy absorption in those FE models are about
602 3.3% and -1.1% respectively compared to that with sealant joints having E of 2.3 MPa.

603 Fig. 18(b) compares the energy absorption of the LG panel for different stiffness of the
604 structural sealant joints under the stronger blast load. The FE model with sealant joints
605 having E of 2.3 MPa absorbs a maximum energy of about 279.1 J and those obtained from
606 the FE models with sealant joints having E of 1.5 and 3.4 MPa are about 284.6 and 273.6 J
607 respectively. The variations of the maximum energy absorption in those FE models are about
608 2% and -2% respectively compared to that with sealant joints having E of 2.3 MPa. The
609 energy absorption time-history curves are similar, but the FE models with sealant joints
610 having a smaller E absorb slightly more energy compared to those with higher E. Overall, it

611 is evident that the E of sealant joints has little impact on the energy absorption of LG panels
612 under the treated blast loads.

613 ***Support reactions (R_L)***

614 Fig. 19(a) compares the variation of the support reaction R_L of the LG panel for different
615 stiffness of the structural sealant joints under the weaker blast load. The FE model with
616 sealant joints having E of 2.3 MPa has a maximum R_L of about 11.3 kN/m and those obtained
617 from the FE models with sealant joints having E of 1.5 and 3.4 MPa are about 10.2 and 11.4
618 kN/m respectively. The variations of the maximum value of R_L in those FE models are about
619 -9.7% and 0.9% respectively compared to that with sealant joints having E of 2.3 MPa.

620 Fig. 19(b) compares the variation of the support reaction R_L of the LG panel for different
621 stiffness of the structural sealant joints under the stronger blast load. The FE model with
622 sealant joints having E of 2.3 MPa has a maximum R_L of about 12.3 kN/m and those obtained
623 from the FE models with sealant joints having E of 1.5 and 3.4 MPa are about 10.8 and 17.7
624 kN/m respectively. The variations of the maximum value of R_L in those FE models are about
625 –12.2% and 43.9% respectively compared to that with sealant joints having E of 2.3 MPa. It
626 is evident that the E of sealant joints has less impact on the R_L under the weaker blast load,
627 but it has some impact on the R_L under the stronger blast load.

628 ## Summary and Conclusion

629 A study on the blast response of LG panels using a comprehensive numerical procedure has
630 been presented. LG panels were modeled with three dimensional (3D) constant stress solid
631 elements incorporating glass, interlayer and structural sealant joints. LG panel with a length
632 of 1.1 m, width of 0.9 m and a thickness of 7.52 mm (3 mm annealed glass + 1.52 mm PVB +
633 3 mm annealed glass) was considered and its performance was investigated under two

different blast loads. According to ASTM F 2248-09 (ASTM 2010a), LG panel should be fixed to the frame using structural silicone sealant joints having a minimum thickness of 5 mm and a width (bite) of 10-12 mm. A parametric study was carried out by varying the width, thickness and the Young's modulus (E) of the structural sealant joints to investigate their effects on the blast performance of the LG panel. Results from FE analysis for mid-span deflection, energy absorption and support reactions under the selected blast loads were presented and discussed.

The width of the structural sealant joints was varied between 7.5-20 mm. The use of wider sealant joints reduces the mid-span deflection and energy absorption of the LG panels, while increasing their support reactions. Results showed that the FE model with 7.5 mm wide sealant joints increases the energy absorption by less than 5% and reduces the support reaction force by less than 10%, showing little improvement compared to that with 10 mm wide sealant joints. FE models with 12.5, 15 and 20 mm wide sealant joints show an increase in the reaction force of 42.3%, 56.1% and 111.4% respectively compared to that with 10 mm wide sealant joints. The use of 10-12 mm wide sealant joints could be a safe and economical solution for the selected LG panel agreeing with the guidelines given in ASTM F 2248-09. Overall, the use of sealant joints with a smaller width could be recommended if they can withstand the design blast load.

The thickness of the structural sealant joints was varied between 4-6 mm. FE models with thinner sealant joints have less flexibility at the supports and hence reduce the mid-span deflection and energy absorption while increasing the support reaction. ASTM F 2248-09 recommends using at least 5 mm thick sealant joints for LG panels designed to be blast resistant. LG panel with 4 mm thick sealant joints shows about 21.1% increase in the support reaction compared to that with 5 mm thick sealant joints under the stronger blast load. FE model with 6 mm thick sealant joints increases the energy absorption less than 4% and

659 reduces the support reaction less than 5%, showing little improvement compared to that with
660 5 mm thick sealant joints under the chosen blast loads. LG panels with thicker sealant joints
661 require window frames with lager dimensions. The use of at least 5 mm thick sealant joints
662 could therefore be recommended supporting the provisions given in ASTM F 2248-09.

663 The Young's modulus (E) of the structural sealant joints was varied between 1.5-3.4 MPa.
664 Sealant joints with smaller E show increases in the mid-span deflection and hence the energy
665 absorption of the LG panel while reducing the support reaction. The E of sealant joints has
666 less impact on the energy absorption, but has a noticeable impact on the support reaction. FE
667 model with sealant joints having E of 3.4 MPa has a reaction force which is about 43.9%
668 higher than that with sealant joints having E of 2.3MPa. Sealant joints with smaller E could
669 be recommended for LG panels, provided that they are able to withstand the design blast load
670 without failure at the supports.

671 The guidelines given in the design standard ASTM F 2248-09 to determine the width and the
672 thickness of the sealant joints agreed well with those predicted from FE analysis. LG panels
673 should be designed to maximize the energy absorption while minimizing the reactions forces
674 transferred to the supporting frames. The present study showed that the width, thickness and
675 the Young's modulus (E) of the sealant joints have a considerable influence on the energy
676 absorption and the support reactions of the LG panels and therefore they should be analyzed
677 carefully when designing LG panels under blast loads. The sealant joints should not be
678 overdesigned using stiffer material or wider joints as they reduce the energy absorption while
679 increasing support reactions. On the other hand they should provide adequate restraint at the
680 supports without failing under the design blast load. The findings of this study will
681 complement and supplement the guidance provided in the current design standards. The
682 information generated in this paper will therefore enable engineers to provide safer and more

683 economical designs of the entire façade system including window glazing, frames and
684 supporting structures.

685

686 ## References

687 ASTM. (2009). "Standard practice for determining load resistance of glass in buildings." *E*
688 *1300-09a*, West Conshohocken, PA.

689 ASTM. (2010a). "Standard practice for specifying an equivalent 3-second duration design
690 loading for blast resistant glazing fabricated with laminated glass." *2248-09 AF*, West
691 Conshohocken, PA.

692 ASTM. (2010b). "Standard test method for glazing and window systems subject to air blast
693 loadings." *1642-04*, West Conshohocken, PA.

694 Chung, J. H., Consolazio, G. R., Dinan. R. J. and Rinehart, S. A. (2010). "Finite - element
695 analysis of fluid - structure interaction in a blast - resistant window system." *J. Struct.*
696 *Eng.*, 136 (3), 297-306.

697 Hallquist, J. O. (2006). "LS-DYNA version 970 theory manual." *Livermore Software*
698 *Technology Corporation*, Livermore, Calif.

699 Hidallana-Gamage, H. D., Thambiratnam, D. P. and Perera, N. J. (2013a). "Computational
700 analysis of laminated glass panels under blast loads: A comparison of two
701 dimensional and three dimensional modeling approaches." *Int. J. Eng. and Sci*., 2(8),
702 69-79.

703 Hidallana-Gamage, H. D., Thambiratnam, D. P. and Perera, N. J. (2013b). "Failure analysis
704 of laminated glass panels subjected to blast loads." *Eng. Failure Anal.*, 36, 14-29.

705 Holmquist, T. J., Johnson, G. R., Lopatin, C., Grady, D. E., Hertel Jr, E. S. (1995). "High
706 strain rate properties and constitutive modeling of glass." Sandia National Labs,
707 Albuquerque, NM , United States.

708 Hooper, P. A., Sukhram, R. A. M., Blackman, B. R. K., and Dear, J. P. (2012). "On the blast
709 resistance of laminated glass." *Int. J. Solids and Struct.*, 49(6), 899-918.

710 International Organization for Standardization (ISO). (1994). "Rubber, vulcanized or
711 thermoplastic: determination of hardness (Hardness between 10 IRHD and 100
712 IRHD)." *ISO 48*, Geneva, Switzerland.

713 International Organization for Standardization (ISO). (2007a). "Glass in building - explosion-
714 resistant security glazing - test and classification for arena air-blast loading." *ISO*
715 *16933*, Geneva, Switzerland.

716 International Organization for Standardization (ISO). (2007b). "Glass in building - explosion
717 resistant security glazing - test and classification by shock tube loading." *ISO 16934*,
718 Geneva, Switzerland.

719 Larcher, M., Solomos, G., Casadei, F. and Gebbeken, N. (2012). "Experimental and
720 numerical investigations of laminated glass subjected to blast loading." *Int. J. Impact*
721 *Eng*., 39(1), 42-50.

722 Ledbetter, S. R., Walker, A. R. and Keiller, A. P. (2006). "Structural use of glass." *J. Archit.*
723 *Eng*., 12(3), 137-149.

724 Lin, L., Hinman, E., Stone, H., and Roberts, A. (2004). "Survey of window retrofit solutions
725 for blast mitigation." *J. Perform. Constr. Facil*., 18(2), 86-94.

726 Ngo, T., Mendis, P., Gupta, A. and Ramsay, J. (2007). "Blast loading and blast effects on
727 structures - An overview." *Electronic J. Struct. Eng*., 7, 76-91.

728 Norville, H. and Conrath, E. (2001). "Considerations for blast-resistant glazing design." *J.*
729 *Archit. Eng.*, 7(3), 80-86.

730 Norville, H., Harvill, N., Conrath, E., Shariat, S., and Mallonee, S. (1999). "Glass-related
731 injuries in Oklahoma city bombing." *J. Perform. Constr. Facil.*, 13(2), 50-56.

732 Seica, M. V., Krynski, M., Walker, M. and Packer, J. A. (2011). "Analysis of dynamic
733 response of architectural glazing subject to blast loading." *J. Archit. Eng.*, 17(2), 59-
734 74.

735 Silva, P. and Lu, B. (2009). "Blast resistance capacity of reinforced concrete slabs." *J. Struct.*
736 *Eng.*, 135(6), 708-716.

737 Teich, M., Warnstedt, P. and Gebbeken, N. (2011). "The influence of negative phase loading
738 on cable net facade response." *J. Archit. Eng.*, 18(4), 276-284.

739 Department of Defense (DOD). (2008). "Structures to resist the effect of accidental
740 explosions." *UFC 3-340-02*, Washington, D. C.

741 Department of Defense (DOD). (2013). "Unified facilities criteria DOD minimum
742 antiterrorism standards for buildings." *UFC 4-010-01*, Washington, D. C.

743 U.K. Glazing Hazard Guide. (1997). "Glazing hazard guide, cubicle stand-offs, tables and
744 charts." SAFE/SSG, Explosive Protection, London, SSG/EP/4/97.

745 Weggel, D. C. and Zapata, B. J. (2008). "Laminated glass curtain walls and laminated glass
746 lites subjected to low-level blast loading." *J. Struct. Eng*., 134(3), 466-477.

747 Wei, J. and Dharani, L. R. (2006). "Response of laminated architectural glazing subjected to
748 blast loading." *Int. J. Impact Eng.*, 32(12), 2032-2047.

Table 1. Material properties and JH-2 material constants of glass used in the FE analyses

Material property/JH-2 constant	Value
Density (ρ)	2530 kg/m^3
Young's modulus (E)	72 GPa
Poisson's ratio (υ)	0.22
Strength constants	
A	0.93
B	0.2
C	0.003
M	1.0
N	0.77
Ref strain rate (EPSI)	1.0
Tensile strength (T)	60 MPa
Failure strain	0.0024
Normalized fractured strength	0.5
HEL	5.95 GPa
HEL pressure	2.92 GPa
HEL strength	4.5 GPa
Damage constants	
D1	0.043
D2	0.85
Equation of state	
K1 (bulk modulus)	45.4 GPa
K2	-138 GPa
K3	290 GPa
β	1.0

Table 2. Material properties of PVB interlayer and silicone sealant used in the FE analyses

Material property	PVB	Rubber
Density (ρ)	1100 kg/m^3	1100 kg/m^3
Young's modulus (E)	530 MPa	2.3 MPa
Poisson's ratio (υ)	0.485	0.495
Yield stress	11 MPa	2.3 MPa
Failure stress	28 MPa	3.5 MPa
Failure strain	2	2.5

Table 3. Comparison of results for different widths (w) of the structural silicone sealant joints

Width (mm)	Maximum Deflection (mm)		Maximum energy absorption (J)		Maximum support reaction (R_L) (kN/m)	
	Blast load 1 (weaker)	Blast load 2 (stronger)	Blast load 1 (weaker)	Blast load 2 (stronger)	Blast load 1 (weaker)	Blast load 2 (stronger)
7.5	33.2 (-2.4%)	131.0 (18.4%)	65.1 (3.0%)	290.4 (4.0%)	10.6 (-6.2%)	11.3 (-8.1%)
10.0	34	110.6	63.2	279.1	11.3	12.3
12.5	32.8 (-3.5%)	100.6 (-9%)	62.4 (-1.3%)	270.6 (-3.0%)	12.6 (11.5%)	17.5 (42.3%)
15.0	32.4 (-4.7%)	98.1 (-11.3%)	62.0 (-1.9%)	268.4 (-3.8%)	12.7 (12.4%)	19.2 (56.1%)
20.0	24.5 (-27.9%)	95.4 (-13.7%)	45.6 (-27.8%)	243.3 (-12.8%)	12.9 (14.2%)	26 (111.4%)

Table 4. Comparison of results for different thicknesses (t) of the structural silicone sealant joints

Thickness (mm)	Maximum Deflection (mm)		Maximum energy absorption (J)		Maximum support reaction (R_L) (kN/m)	
	Blast load 1 (weaker)	Blast load 2 (stronger)	Blast load 1 (weaker)	Blast load 2 (stronger)	Blast load 1 (weaker)	Blast load 2 (stronger)
4	32.8 (-3.5%)	103.7 (-6.2%)	62.6 (-0.9%)	273.8 (-1.9%)	12.8 (13.3%)	14.9 (21.1%)
5	34	110.6	63.2	279.1	11.3	12.3
6	35.7 (5%)	117.1 (5.9%)	64.5 (2.1%)	288.1 (3.2%)	10.8 (-4.4%)	12.1 (-1.6%)

Table 5. Comparison of results for different Young's moduli (E) of the structural silicone sealant joints

Young's modules (MPa)	Maximum Deflection (mm)		Maximum energy absorption (J)		Maximum support reaction (R_L) (kN/m)	
	Blast load 1 (weaker)	Blast load 2 (stronger)	Blast load 1 (weaker)	Blast load 2 (stronger)	Blast load 1 (weaker)	Blast load 2 (stronger)
1.5	35 (2.9%)	113.8 (2.9%)	65.3 (3.3%)	284.6 (2.0%)	10.2 (-9.7%)	10.8 (-12.2%)
2.3	34	110.6	63.2	279.1	11.3	12.3
3.4	33.4 (-1.8%)	103.7 (-6.2%)	62.5 (-1.1%)	273.6 (-2.0%)	11.4 (0.9%)	17.7 (43.9%)

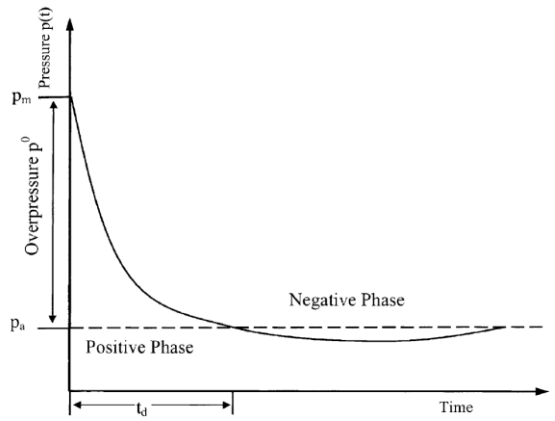

Fig 1. Blast overpressure variation with the time for a typical blast load (Wei et al. 2006)

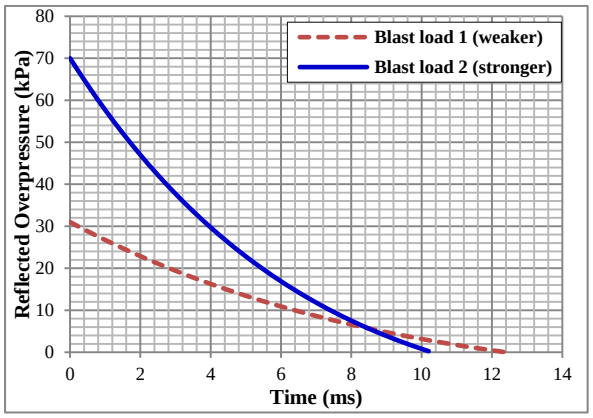

Fig. 2. Reflected overpressure variation of the blast loads

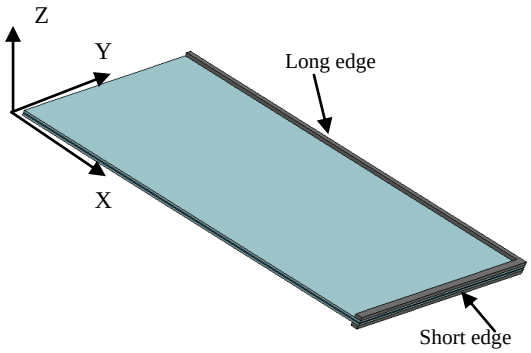

(a) 3D view

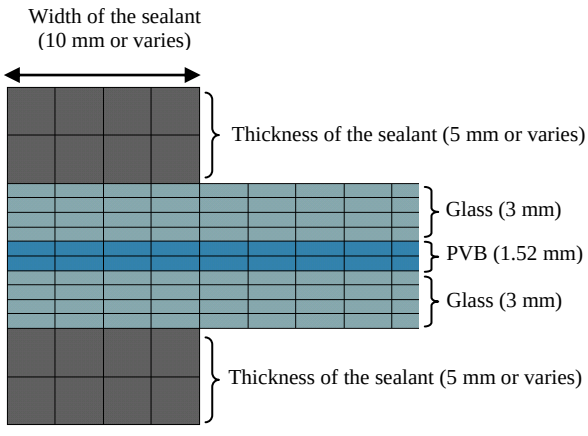

(b) Sectional view at the support

Fig. 3. FE model of the LG panel

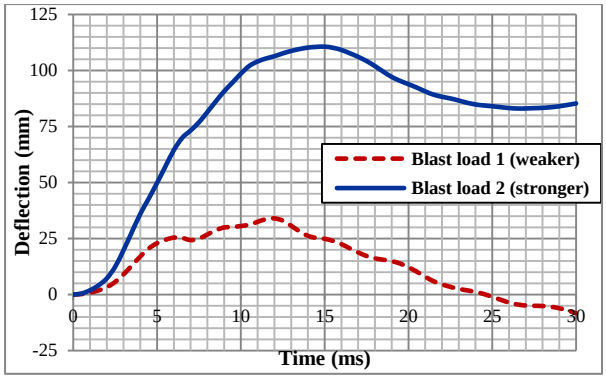

Fig. 4. Mid-span deflection variation under the blast loads

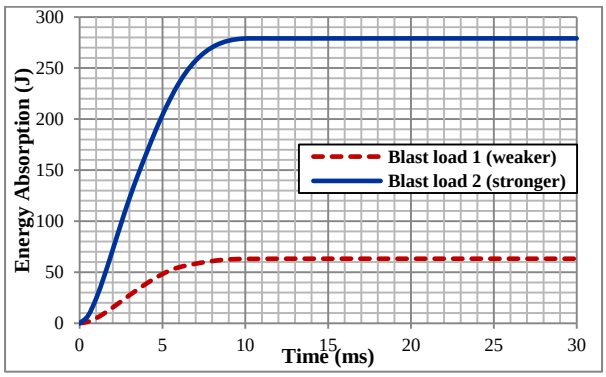

Fig. 5. Energy absorption variation under the blast loads

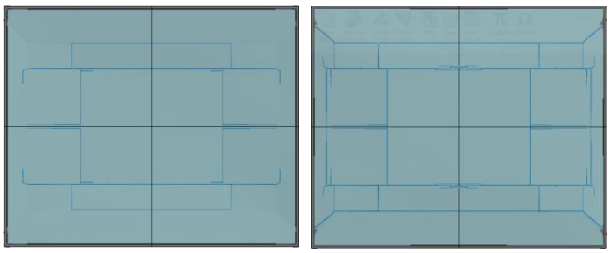

(a) front glass pane (b) back glass pane

Fig. 6. Crack propagation of glass panes under the weaker blast load at 12 ms

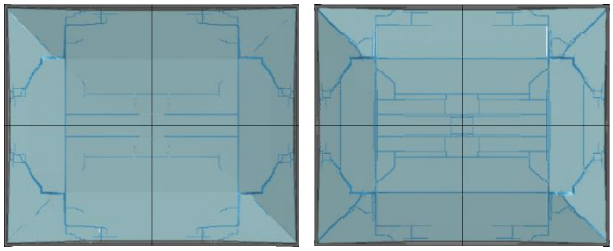

(a) front glass pane (b) back glass pane

Fig. 7. Crack propagation of glass panes under the stronger blast load at 15 ms

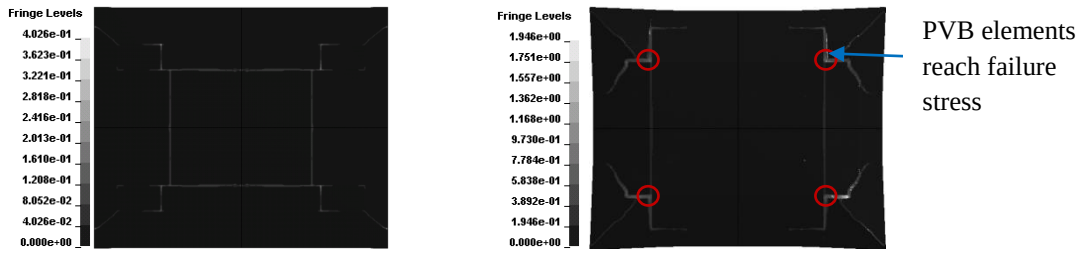

(a) under weaker blast load at 12 ms (b) under stronger blast load at 15 ms

Fig. 8. Plastic strain variation on the bottom surface of the interlayer

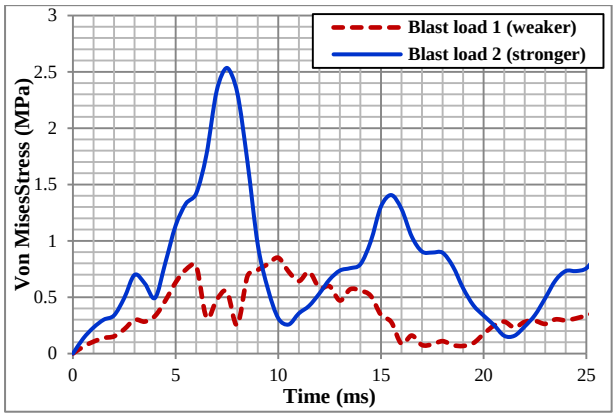

Fig. 9. Von mises stress (σ_v) variation in critical sealant elements at the middle of the long edge

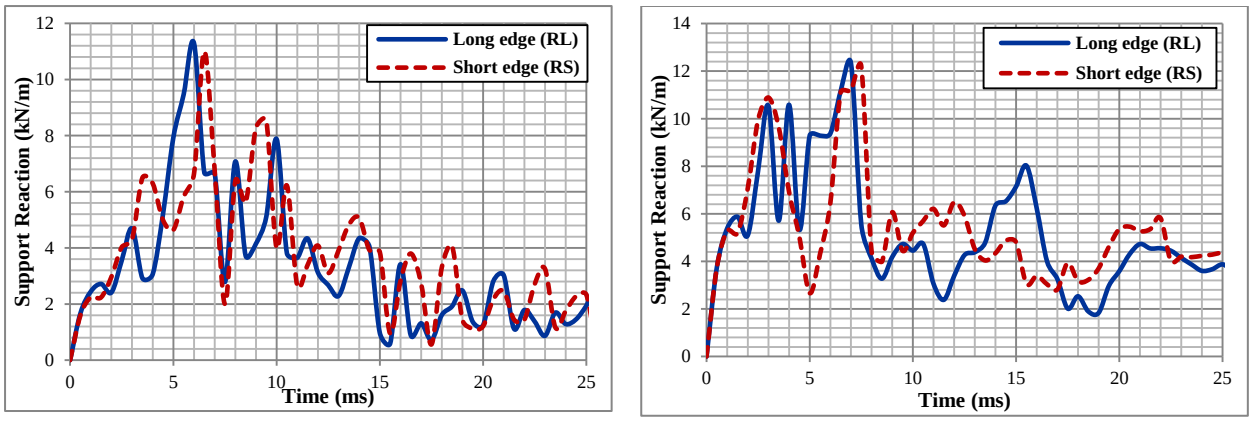

(a) under weaker blast load (b) under stronger blast load

Fig. 10. Comparison of the support reactions at the middle of the long and short edges

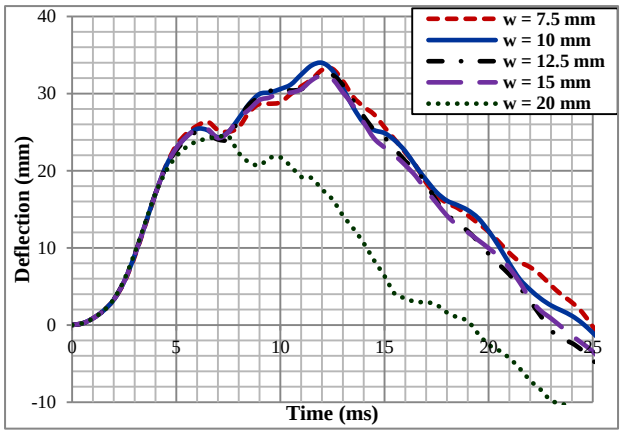

(a) under weaker blast load

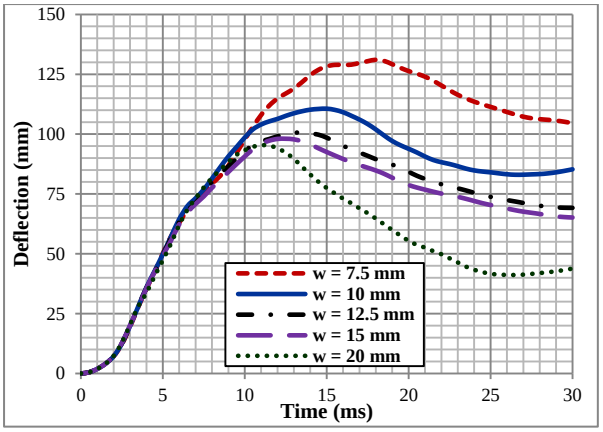

(b) under stronger blast load

Fig. 11. Mid-span deflection of the LG panel for different widths (w) of sealant joints (thickness and E of sealant joints are 5 mm and 2.3 MPa respectively)

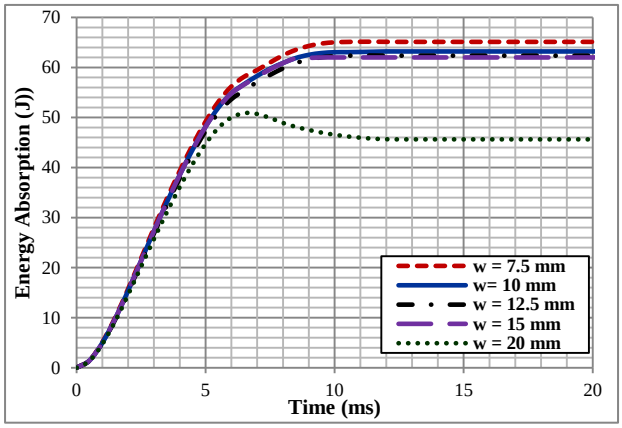

(a) under weaker blast load

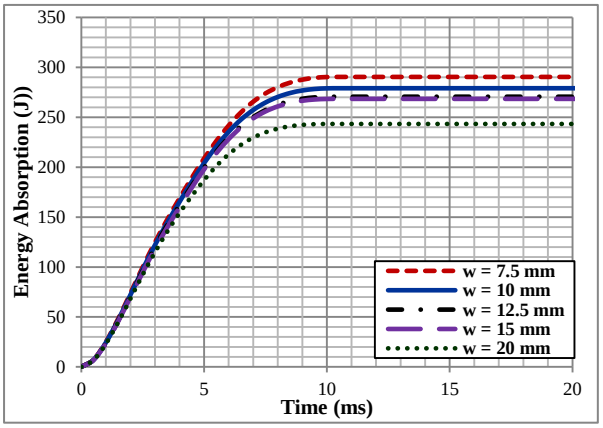

(b) under stronger blast load

Fig. 12. Energy absorption of the LG panel for different widths (w) of sealant joints (thickness and E of sealant joints are 5 mm and 2.3 MPa respectively)

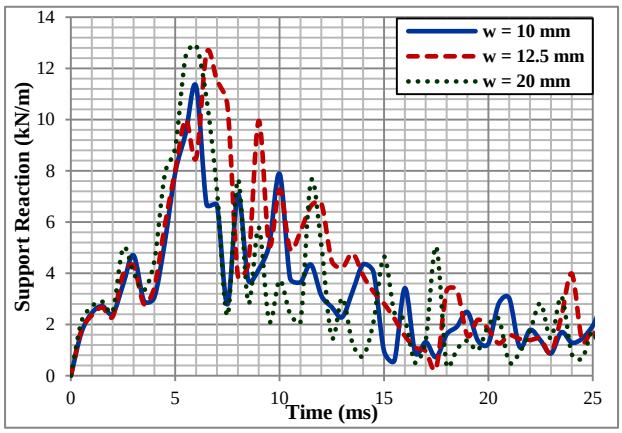

(a) under weaker blast load

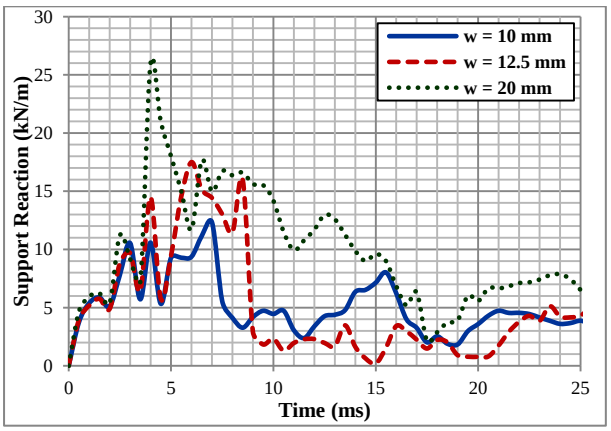

(b) under stronger blast load

Fig. 13. Support reaction, R_L of the LG panel for different widths (w) of sealant joints (thickness and E of sealant joints are 5 mm and 2.3 MPa respectively)

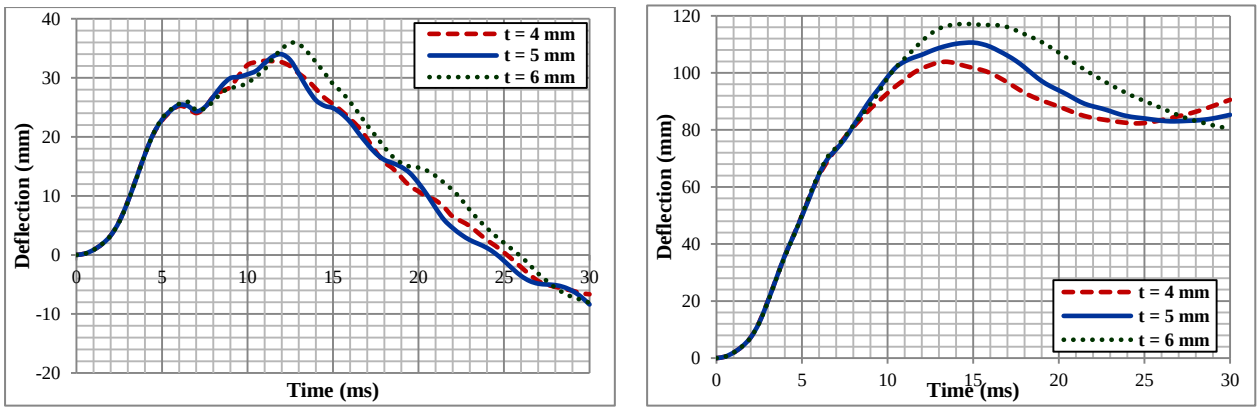

(a) under weaker blast load (b) under stronger blast load

Fig. 14. Mid-span deflection of the LG panel for different thicknesses (t) of sealant joints (width and E of sealant joints are 10 mm and 2.3 MPa respectively)

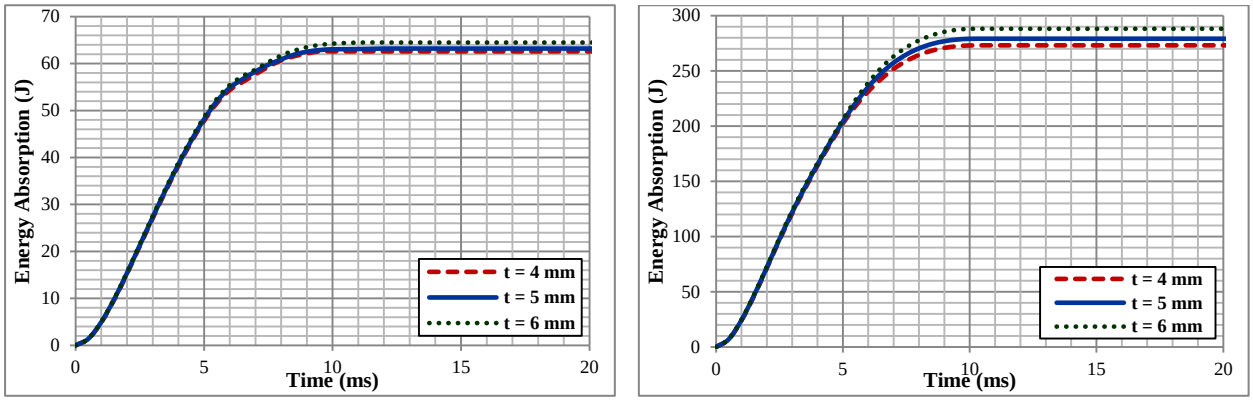

(a) under weaker blast load (b) under stronger blast load

Fig. 15. Energy absorption of the LG panel for different thicknesses (t) of sealant joints (width and E of sealant joints are 10 mm and 2.3 MPa respectively)

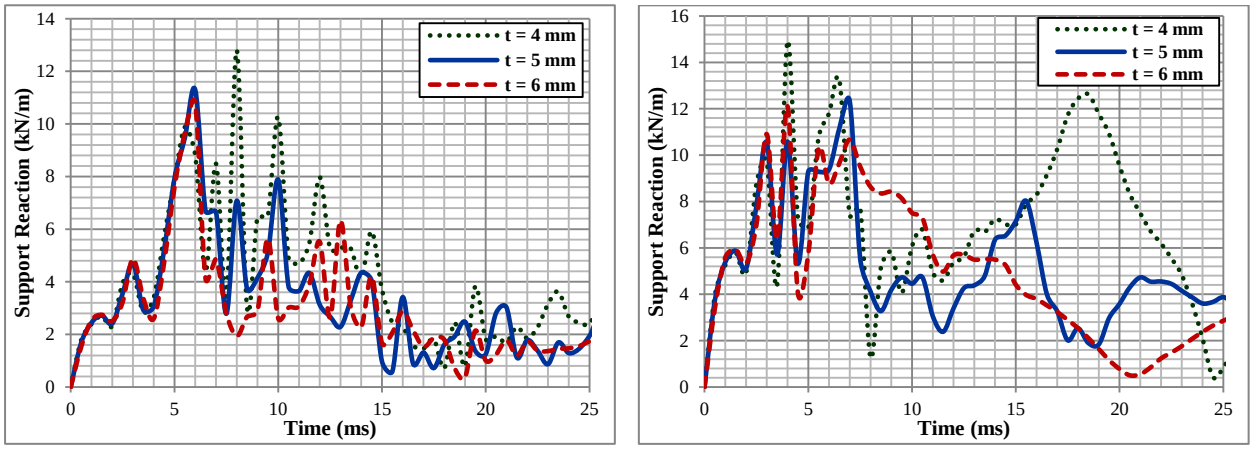

(a) under weaker blast load (b) under stronger blast load

Fig. 16. Support reaction, R_L of the LG panel for different thicknesses (t) of sealant joints (width and E of sealant joints are 10 mm and 2.3 MPa respectively)

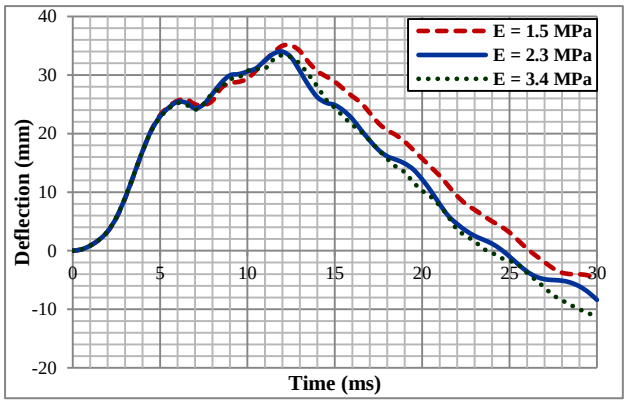

(a) under weaker blast load

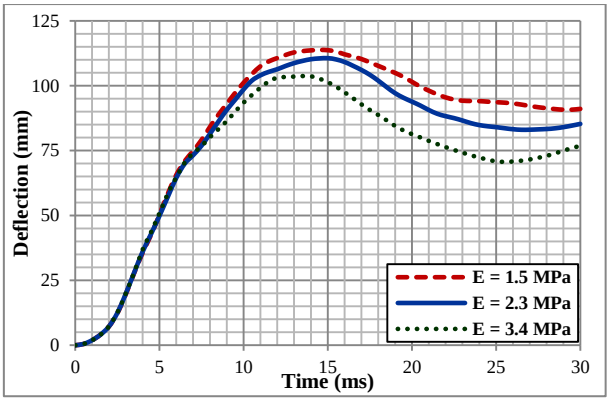

(b) under stronger blast load

Fig. 17. Mid-span deflection of the LG panel for different Young's moduli (E) of sealant joints (width and thickness of sealant joints are 10 and 5 mm respectively)

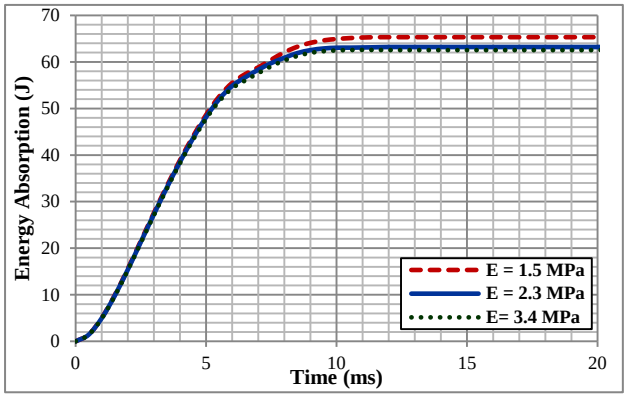

(a) under weaker blast load

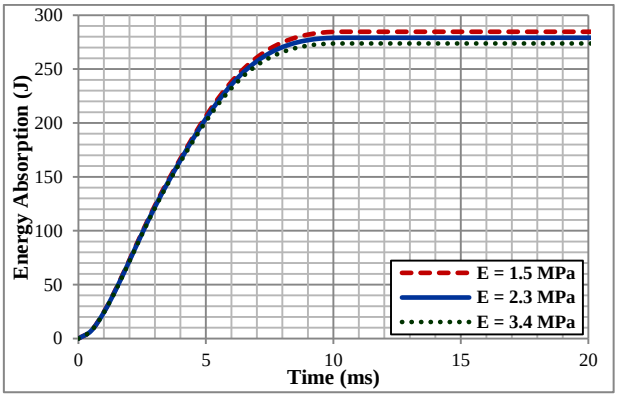

(b) under stronger blast load

Fig. 18. Energy absorption of the LG panel for different Young's moduli (E) of sealant joints (width and thickness of sealant joints are 10 and 5 mm respectively)

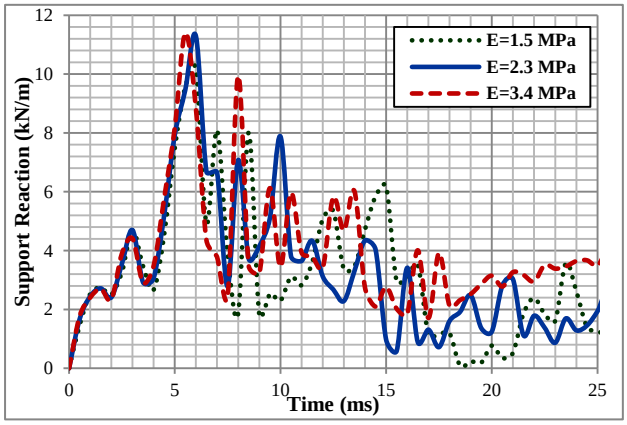

(a) under weaker blast load

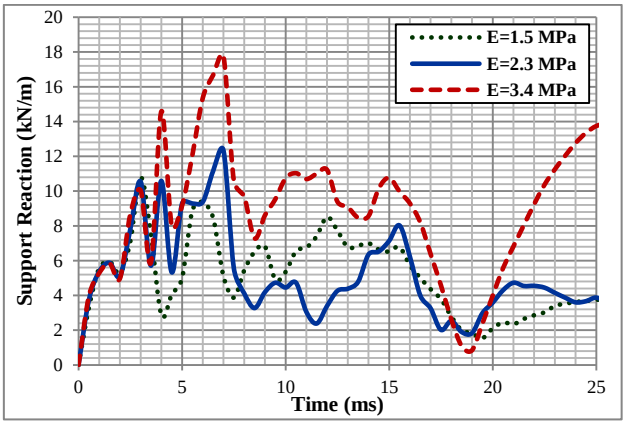

(b) under stronger blast load

Fig. 19. Support reaction, R_L of the LG panel for different Young's moduli (E) of sealant joints (width and thickness of sealant joints are 10 and 5 mm respectively)